J|A|C|S ARTICLES

Published on Web 04/15/2010

Lysine and Arginine Side Chains in Glycosaminoglycan−Protein Complexes Investigated by NMR, Cross-Linking, and Mass Spectrometry: A Case Study of the Factor H−Heparin Interaction

Bärbel S. Blaum,[†] Jon A. Deakin,[‡] Conny M. Johansson,[†] Andrew P. Herbert,[†] Paul N. Barlow,[†] Malcolm Lyon,[‡] and Dušan Uhrín*,[†]

Edinburgh Biomolecular NMR Unit, School of Chemistry and School of Biological Sciences, University of Edinburgh, West Mains Road, Edinburgh EH9 3JJ, Scotland, United Kingdom, and Cancer Research UK Glyco-Oncology Group, School of Cancer and Imaging Sciences, Paterson Institute for Cancer Research, University of Manchester, Wilmslow Road, Manchester M20 4BX, United Kingdom

Received January 4, 2010; E-mail: dusan.uhrin@ed.ac.uk

Abstract: We have used the interaction between module 7 of complement factor H (CFH∼7) and a fully sulfated heparin tetrasaccharide to exemplify a new approach for studying contributions of basic side chains to the formation of glycosaminoglycan (GAG)−protein complexes. We first employed HISQC and H_2CN NMR experiments to monitor the side-chain resonances of lysines and arginines in ^{15}N, ^{13}C-labeled protein during titrations with a fully sulfated heparin tetrasaccharide under physiological conditions. Under identical conditions and using ^{15}N-labeled protein, we then cross-linked tetrasaccharide to CFH∼7 and confirmed the 1:1 stoichiometry by FT-ICR-MS. We subsequently characterized this covalent protein−GAG conjugate by NMR and further MS techniques. MALDI-TOF MS identified protein fragments obtained via trypsin digestion or chemical fragmentation, yielding information concerning the site of GAG attachment. Combining MS and NMR data allowed us to identify the side chain of K405 as the point of attachment of the cross-linked heparin oligosaccharide to CFH∼7. On the basis of the analysis of NMR and MS data of the noncovalent and cross-linked CFH∼7−tetrasaccharide complexes, we conclude that the K446 side chain is not essential for binding the tetrasaccharide, despite the large chemical shift perturbations of its backbone amide ^{15}N and ^{1}H resonances during titrations. We show that R444 provides the most important charge−charge interaction within a C-terminal heparin-binding subsite of CFH∼7 whereas side chains of R404, K405, and K388 are the predominant contributors to an N-terminal binding subsite located in the immediate vicinity of residue 402, which is implicated in age-related macular degeneration (AMD).

Introduction

Glycosaminoglycans (GAGs) are linear polysaccharides found ubiquitously on animal cell surfaces and in the extracellular matrix. GAGs usually occur linked to protein cores as proteoglycans and in most cases accomplish their biological functions through interactions with ligand proteins.[1−4] Such interactions have a strong electrostatic component mediated by the negatively charged functional groups of GAGs (sulfates, sulfonamides, and carboxyl groups) and positively charged amino acid side chains of proteins (lysines, arginines, and occasionally histidines). In enzymes that are involved in GAG biosynthesis and degradation, GAGs bind in deep canyons and clefts.[5] In complexes with growth factors, however, GAGs often sit in shallow grooves on protein surfaces,[6−8] making these interactions less specific than protein−protein interactions. Charge density, rather than a requirement for a specific structural motif, is often sufficient for complex formation.[9−11] A well-documented exception is the interaction of a heparin pentasaccharide with antithrombin III, which requires a very specific GAG motif.[12,13]

[†] University of Edinburgh.
[‡] University of Manchester.

(1) Gandhi, N. S.; Mancera, R. L. *Chem. Biol. Drug Des.* **2008**, *72*, 455–482.
(2) Bishop, J. R.; Schuksz, M.; Esko, J. D. *Nature* **2007**, *446*, 1020–1027.
(3) Imberty, A.; Lortat-Jacob, H.; Perez, S. *Carbohydr. Res.* **2007**, *342*, 439–439.
(4) Sasisekharan, R.; Raman, R.; Prabhakar, V. *Annu. Rev. Biomed. Eng.* **2006**, *8*, 181–231.
(5) Moon, A. F.; Edavettal, S. C.; Krahn, J. M.; Munoz, E. M.; Negishi, M.; Linhardt, R. J.; Liu, J.; Pedersen, L. C. *J. Biol. Chem.* **2004**, *279*, 45185–45193.
(6) DiGabriele, A. D.; Lax, I.; Chen, D. I.; Svahn, C. M.; Jaye, M.; Schlessinger, J.; Hendrickson, W. A. *Nature* **1998**, *383*, 812–817.
(7) Faham, S.; Hileman, R. E.; Fromm, J. R.; Linhardt, R. J.; Rees, D. C. *Science* **1996**, *271*, 1116–1120.
(8) Lietha, D.; Chirgadze, D. Y.; Mulloy, B.; Blundell, T. L.; Gheradi, E. *EMBO J.* **2001**, *20*, 5543–55.
(9) Kreuger, J.; Spillmann, D.; Li, J. P.; Lindahl, U. *J. Cell Biol.* **2006**, *174*, 323–327.
(10) Lindahl, U. *Thromb. Haemost.* **2007**, *98*, 109–115.
(11) Deakin, J. A.; Blaum, B. S.; Gallagher, J. T.; Uhrín, D.; Lyon, M. *J. Biol. Chem.* **2009**, *284*, 6311–6321.
(12) Lindahl, U.; Backstrom, G.; Thunberg, L.; Leder, I. G. *Proc. Natl. Acad. Sci. U.S.A.* **1980**, *77*, 6551–6555.

 10.1021/ja1000517

Nonetheless, GAG composition varies depending on the type and developmental stage of the tissue in which they are expressed,[14−16] hinting at the functional relevance of subtle structural variations. Indeed, changes in GAG structure and composition have been identified as possible biomarkers for cancer.[17,18] Developing new methods for the characterization of protein−GAG complexes[19] is therefore important to our understanding of the biological roles of GAGs and essential to realizing their therapeutic potential.[10]

The growing awareness of the role played by heparan sulfate (HS) in cell−cell communication and the potential applications of cross-linked heparin−protein conjugates for medical purposes underline the importance of the structural elucidation of such constructs. HS/heparin chains cross-linked to protein are likely to be more stable to enzymatic degradation than free GAGs. Covalent protein−GAG conjugates may also be more potent in the formation of ternary complexes, such as with signaling receptors, than transient, noncovalent protein−GAG complexes.[20] Recently, a synthetic CD4-HS glycoconjugate was shown to inhibit CCR5- and CXCR4-mediated HIV-1 attachment and viral entry.[21]

In this study we present novel approaches to the characterization of noncovalent protein−GAG complexes and covalently cross-linked protein−GAG conjugates in solution by a combination of NMR spectroscopy and mass spectrometry. Our methodology is illustrated using the interaction between HS and module 7 of human complement factor H (CFH∼7). Mature HS contains variably sulfated domains interrupted by domains essentially lacking sulfation,[22] and typically proteins bind to the highly sulfated domains.[23] Consequently, heparin, which shares an identical carbohydrate skeleton with HS but displays a higher and more evenly distributed level of sulfation, is often used in structural studies as an HS mimetic, as is the case in the present study.

CFH, the main fluid-phase regulator of the alternative pathway of the complement,[24] is a 155 kDa heparin-binding protein consisting of twenty ∼7 kDa complement control protein modules (CCPs). CCPs have a prolate ellipsoid shape, a high β-sheet content, and two conserved disulfide bonds per module. They are connected by linkers of 3−8 residues, giving CFH the appearance of 20 beads on a string. By binding to HS or other cell-surface polyanions,[25] CFH protects host cells from complement attack.[26,27] This interaction is thought to lie at the center of host-cell protection from the innate immune system and is particularly important for cells lacking alternative membrane-bound regulators.

The Y402H single nucleotide polymorphism in CFH∼7, present in about 30% of the population, is associated (in homozygous individuals) with a 7-fold increase in the occurrence of age-related macular degeneration (AMD).[28−31] Because CFH∼7 contributes directly to one of the two principal heparin-binding sites in CFH, it was proposed that a change in polyanion-binding properties of the histidine allotype compromises the ability of CFH to protect the Bruch's membrane from complement-mediated damage. This membrane underlies the retinal pigment epithelium, and its damage triggers inflammatory processes eventually leading to AMD onset.[32] In this study we have used the Y402 variant, which is referred to from now on as CFH∼7. Solution structures of both variants of CFH∼7 have been previously solved by NMR.[33] The crystal structure of disease-linked variant H402, in the context of triple module CFH∼6−8 complexed with sucrose octasulfate (SOS), has also been determined previously.[34]

Protein−GAG interactions are typically weak and fall into the fast-exchange regime on the NMR timescale. This facilitates the tracking of ligand-induced chemical shift perturbations in $^{1}H-^{15}N$-HSQC spectra of ^{15}N-labeled proteins through chemical-shift averaging of free and bound proteins. However, such an analysis is generally limited to backbone NH resonances. A lack of chemical shift perturbations of the backbone NH atoms belonging to basic residues is a poor indicator of the noninvolvement of their side chains in GAG binding whereas, vice versa, changes in backbone NH chemical shifts do not necessarily imply the involvement of the corresponding arginine and lysine side chains. To complement backbone NH chemical shift perturbation data, we monitored lysine $N^{\zeta}H^{\zeta}{}_{3}^{+}$ and arginine $N^{\varepsilon}H^{\varepsilon}$ resonances during GAG titrations. In addition, we used chemical cross-linking as a means to probe the roles of individual lysine side chains in the formation of protein−GAG complexes. We employed a zero-length cross-linking technique, originally designed to cross-link proteins through contacts between primary amino and carboxylate groups.[35] This methodology couples the amino group of a lysine side chain to the activated carboxylate

(13) Choay, J.; Petitou, M.; Lormeau, J. C.; Sinay, P.; Casu, B.; Gatti, G. *Biochem. Biophys. Res. Commun.* **1983**, *116*, 492–499.
(14) Kato, M.; Wang, H.; Bernfield, M.; Gallagher, J. T.; Turnbull, J. E. *J. Biol. Chem.* **1994**, *269*, 18881–18890.
(15) Feyzi, E.; Saldeen, T.; Larsson, E.; Lindahl, U.; Salmivirta, M. *J. Biol. Chem.* **1998**, *273*, 13395–13398.
(16) Tissot, B.; Gasiunas, N.; Powell, A. K.; Ahmed, Y.; Zhi, Z. L.; Haslam, S. M.; Morris, H. R.; Turnbull, J. E.; Gallagher, J. T.; Dell, A. *Glycobiology* **2007**, *17*, 972–982.
(17) Molist, A.; Romarís, M.; Lindahl, U.; Villena, J.; Touab, M.; Bassols, A. *Eur. J. Biochem.* **1998**, *254*, 371–377.
(18) Blackhall, F. H.; Merry, C. L. R.; Davies, E. J.; Jayson, G. C. *Br. J. Cancer* **2001**, *85*, 1094–1098.
(19) Powell, A. K.; Yates, E. A.; Fernig, D. G.; Turnbull, J. E. *Glycobiology* **2004**, *14*, 17–30.
(20) Parmar, N.; Berry, L. R.; Post, M.; Chan, A. K. *J. Physiol. Lung Cell Mol. Physiol.* **2009**, *296*, L394–L403.
(21) Baleux, F.; Loureiro-Morais, L.; Hersant, Y.; Clayette, P.; Arenzana-Seisdedos, F.; Bonnaffé, D.; Lortat-Jacob, H. *Nat. Chem. Biol.* **2009**, *5*, 743–748.
(22) Murphy, K. J.; Merry, C. L. R.; Lyon, M.; Thompson, J. E.; Roberts, I. S.; Gallagher, J. T. *J. Biol. Chem.* **2004**, *279*, 27239–27245.
(23) Lyon, M.; Gallagher, J. T. *Matrix Biol.* **1998**, *17*, 485–493.
(24) Weiler, J. M.; Daha, M. R.; Austen, K. F.; Fearon, D. T. *Proc Natl. Acad. Sci. U.S.A.* **1976**, *73*, 3268–3272.
(25) Lehtinen, M. J.; Rops, A. L.; Isenman, D. E.; van der Vlag, J.; Jokiranta, T. S. *J. Biol. Chem.* **2009**, *284*, 15650–15658.
(26) Ferreira, V. P.; Herbert, A. P.; Hocking, H. G.; Barlow, P. N.; Pangburn, M. K. *J. Immunol.* **2006**, *177*, 6308–6316.
(27) Pangburn, M. K. *J. Immunol.* **2002**, *169*, 4702–4706.
(28) Klein, R. J.; Zeiss, C.; Chew, E. Y.; Tsai, J. Y.; Sackler, R. S.; Haynes, C.; Henning, A. K.; SanGiovanni, J. P.; Mane, S. M.; Mayne, S. T.; Bracken, M. B.; Ferris, F. L.; Ott, J.; Barnstable, C.; Hoh, J. *Science* **2005**, *308*, 385–389.
(29) Edwards, A. O.; Ritter, R., III.; Abel, K. J.; Manning, A.; Panhuysen, C.; Farrer, L. A. *Science* **2005**, *308*, 421–424.
(30) Haines, J. L.; Hauser, M. A.; Schmidt, S.; Scott, W. K.; Olson, L. M.; Gallins, P.; Spencer, K. L.; Kwan, S. Y.; Noureddine, M.; Gilbert, J. R.; Schnetz-Boutaud, N.; Agarwal, A.; Postel, E. A.; Pericak-Vance, M. A. *Science* **2005**, *308*, 419–421.
(31) Hageman, G. S.; et al. *Proc. Natl. Acad. Sci. U.S.A.* **2005**, *102*, 7227–7232.
(32) Lotery, A.; Trump, D. *Hum. Genet.* **2007**, 219–236.
(33) Herbert, A. P.; Deakin, J. A.; Schmidt, C. Q.; Blaum, B. S.; Egan, C.; Ferreira, V. P.; Pangburn, M. K.; Lyon, M.; Uhrín, D.; Barlow, P. N. *J. Biol. Chem.* **2007**, *282*, 18960–18968.
(34) Prosser, B. E.; Johnson, S.; Roversi, P.; Herbert, A. P.; Blaum, B. S.; Tyrrell, J.; Jowitt, T. A.; Clark, S. J.; Tarelli, E.; Uhrín, D.; Barlow, P. N.; Sim, R. B.; Day, A. J.; Lea, S. M. *J. Exp. Med.* **2007**, *204*, 2277–2283.
(35) Grabarek, Z.; Gergely, J. *Anal. Biochem.* **1990**, *185*, 131–135.

of a GAG oligosaccharide.[36−39] Assuming that the binding mode of the activated carbohydrate is similar to that of the unmodified oligosaccharide, the formation of an amide bond provides evidence of spatial proximity between a specific lysine side chain and a carboxyl group of the oligosaccharide.

Experimental Section

Preparation of Fully Sulfated Heparin Tetrasaccharide. Fully sulfated tetrasaccharide ΔUA(2S)-GlcNS(6S)-IdoA(2S)-GlcNS(6S) was produced by controlled, partial heparinase I digestion of low-molecular-weight heparin and subsequent purification by gel filtration and ion-exchange chromatography as described previously.[33] The purity was checked by ^{1}H NMR, and concentrations were determined using absorbance at 232 nm with a molar absorption coefficient of 5200 M^{-1} cm^{-1}.[40]

Preparation of CFH∼7. A protein construct containing CFH residues 386−446 (Y402) was cloned into *Pichia pastoris* expression vector pPICZαB (Invitrogen) and transformed into *P. pastoris* strain KM71H (Invitrogen). ^{15}N-labeled protein was expressed in baffled shaker flasks or a Bioflow 3000 fermenter using $(NH_4)_2SO_4$ as the sole nitrogen source. CFH∼7 was purified from the supernatant using cation-exchange chromatography at pH 6.0.[33] The purity was checked by SDS-PAGE and MALDI-TOF MS. The protein consisted of a major fraction with N-terminal truncated artifact EAAG and a minor fraction with full artifact EAEAAG. The former component could readily be purified on a Mono-S cation-exchange column (GE Healthcare) using 20 mM potassium phosphate at pH 6.0 and a linear gradient to 1 M NaCl. ^{13}C, ^{15}N-labeled CFH∼7, as prepared previously,[33] was also used in this study. Protein concentrations were determined using absorbance at 280 nm (calculated extinction coefficient = 13 200 M^{-1} cm^{-1}).

Zero-Length Cross-Linking of a Protein−GAG Complex.[35] Desalted, fully sulfated heparin tetrasaccharide (0.2 mg), 22 mM 1-ethyl-3-[3-dimethylaminopropyl]-carbodiimide hydrochloride (EDC), and 30 mM sulfo-*N*-hydroxysuccinimide (sulfo-NHS) in a total volume of 1 mL of 50 mM 2-(*N*-morpholino)ethanesulfonic acid (MES) at pH 6.0 were incubated at 25 °C for 15 min. The activated tetrasaccharide was recovered from the cross-linking reagents by quick passage over a PD-10 desalting column (GE Healthcare) and immediately mixed with 2.3 mg of CFH∼7 in 1 mL of 50 mM Tris-HCl at pH 6.0. The cross-linking reaction mixture was incubated at 25 °C for 3 h before purification by cation-exchange chromatography on a Mono-S column (GE Healthcare) with 20 mM potassium phosphate at pH 6.0 as the running buffer. The free protein was bound to the column while anionic, cross-linked protein−GAG was collected in the flow-through. Mono-cross-linking was confirmed by MS after buffer exchange into 50 mM ammonium acetate at pH 4.5 using TubeODialyzers (G Biosciences) with an M_r cutoff of 1 kDa.

NMR Experiments. All NMR experiments, with the exception of ^{15}N-relaxation measurements, were conducted on a 600 MHz Bruker AVANCE spectrometer equipped with a 5 mm cryogenic probe. Heteronuclear in-phase single-quantum coherence (HISQC)[41] spectra of free and cross-linked protein were collected in 20 mM potassium phosphate (pH 3.0) at 283 K on a uniformly ^{15}N-labeled sample of 50 μM CFH∼7. HISQC spectra were acquired using a coaxial NMR tube with the capillary (Norell) filled with D_2O to avoid proton−deuterium exchange. The ^{15}N offset was set to 33 ppm, and a spectral width of 5 ppm was used in the indirectly detected dimension. A 900 μs 180° ^{15}N rSNOB pulse[42] was applied during the final refocusing period. Typically, 64 increments were acquired in the ^{15}N dimension, resulting in an acquisition time of 106 ms in t_1. Spectra were typically acquired in <1 h. Assignment of the lysine $N^{\zeta}H^{\zeta}{}_3{}^+$ cross-peaks was accomplished by collecting an (H)CCENH$_3$[41] spectrum on a 0.5 mM sample of free, uniformly ^{13}C- and ^{15}N-labeled CFH∼7 in 20 mM potassium phosphate (pH 3.0) at 283 K and comparing the $C^{\alpha}-C^{\varepsilon}$ chemical shifts with a previously assigned (H)C(CO)NH-TOCSY spectrum[33,43] collected at pH 5.2 (20 mM sodium acetate) and 298 K (Figure 1S). A titration of 0.1 mM ^{13}C, ^{15}N-CFH∼7 with the heparin tetrasaccharide was conducted in 20 mM potassium phosphate (pH 7.4) at 298 K using protein/GAG molar ratios of 1:0, 1:0.5, 1:1, and 1:2 and monitored by 2D H_2CN experiments.[44] ^{15}N and ^{13}C offsets of 33 and 42 ppm were used. All ^{15}N pulses were nonselective. A 1500 μs 180° ^{13}C reBURP pulse[45] was applied during the final refocusing period. Typically, 64 or 32 increments were acquired in the ^{15}N or ^{13}C dimension, resulting in acquisition times of 106 and 21 ms. Two-dimensional ^{15}N and ^{13}C planes were acquired in 2.5 and 1 h, respectively. Lysine cross-peaks were assigned using the N^{ζ} chemical shifts, as obtained for the HISQC spectra, and transferred with the help of further 2D H_2CN spectra collected at intermediate temperatures and pH values. ^{1}H−^{15}N HSQC spectra were acquired using standard parameters and a ^{15}N offset of 120 ppm. The evaluation and assignment of the protein NMR spectra were done using CcpNmr Analysis.[46] ^{15}N relaxation data were acquired on an 800 MHz NMR instrument equipped with a 5 mm cryogenic probe using 25 μM CFH∼7 and 40 μM tetrasaccharide in 20 mM sodium acetate (pH 5.0) at 298 K. The intensities of individual cross-peaks, obtained by deconvolution of the NH signals in the Bruker TOPSPIN program, were fit to an exponential decay in Gnuplot.

Trypsin Digestion. Samples of 65 μg CFH∼7, either free or as cross-linked conjugate, were treated with 0.25 mM dithiothreiol (DTT) and 8 M urea in a total volume of 400 μL and incubated at 75 °C for 1 h. The unfolded and reduced samples were alkylated by incubation with 125 mM iodoacetamide at room temperature (total volume 500 μL). Dialysis into 50 mM ammonium acetate at pH 7.4 was conducted overnight before 2.5 μg of trypsin (sequencing grade, Promega) was added in a volume of 500 μL. Digestion proceeded at 37 °C for 1.5 h and trypsin was then reversibly deactivated by reducing the pH to 4.0 with 1 M acetic acid and cooling the samples to 4 °C. MALDI-TOF MS was used to assess the degree of digestion. For complete digestion, trypsin was reactivated by raising the sample pH to 8.2 and incubating overnight at 37 °C.

Microwave-Assisted Acid Hydrolysis. A cross-linked conjugate (30 μL of 80 μM) was mixed with 0.1 mM DTT and 20% trifluoroacetic acid (TFA) in a total volume of 50 μL in a 1.5 mL Eppendorf microcentrifuge tube.[47] The sample was placed within a glass beaker in a domestic microwave oven, along with a second glass beaker containing roughly 100 mL of water for the absorption of excess radiation and heated with 950 W for 6 min in 2 min steps. After each step, the sample was opened to release the pressure. The sample was then subjected to MALDI-TOF MS. Web

(36) Lyon, M.; Deakin, J. A.; Gallagher, J. T. *J. Biol. Chem.* **2002**, *277*, 1040–1046.
(37) Lau, E. K.; Paavola, C. D.; Johnson, Z.; Gaudry, J. P.; Geretti, E.; Borlat, F.; Kungl, A. J.; Proudfoot, A. E.; Handel, T. M. *J. Biol. Chem.* **2004**, *279*, 22294–22305.
(38) Vivès, R. R.; Crublet, E.; Andrieu, J. P.; Gagnon, J.; Rousselle, P.; Lortat-Jacob, H. *J. Biol. Chem.* **2004**, *279*, 54327–54333.
(39) Vivès, R. R.; Sadir, R.; Imberty, A.; Rencurosi, A.; Lortat-Jacob, H. *Biochemistry* **2002**, *41*, 14779–14789.
(40) Linhardt, R. J.; Rice, K. G.; Kim, Y. S.; Lohse, D. L.; Wang, H. M.; Loganathan, D. *Biochem. J.* **1988**, *254*, 781–787.
(41) Iwahara, J.; Jung, Y. S.; Clore, G. M. *J. Am. Chem. Soc.* **2007**, *129*, 2971–2980.
(42) Kupèe, E.; Boyd, J.; Campbell, I. D. *J. Magn. Reson., Ser. B* **1995**, *106*, 300–303.
(43) Grzesiek, S.; Bax, A. *J. Biomol. NMR* **1993**, *3*, 185–204.
(44) André, I.; Linse, S.; Mulder, F. A. *J. Am. Chem. Soc.* **2007**, *129*, 15805–15813.
(45) Geen, H.; Freeman, R. *J. Magn. Reson.* **1991**, *93*, 91–141.
(46) Vranken, W. F.; Boucher, W.; Stevens, T. J.; Fogh, R. H.; Pajon, A.; Llinas, M.; Ulrich, E. L.; Markley, J. L.; Ionides, J.; Laue, E. D. *Proteins* **2005**, *59*, 687–696.
(47) Zhong, H.; Marcus, S. L.; Li, L. *J. Am. Soc. Mass. Spectrom.* **2005**, *16*, 471–481.

server ProSight PTM (https://prosightptm.scs.uiuc.edu/) was used to assist in peptide identification.

Mass Spectrometry. MALDI-TOF spectra were acquired on a Voyager-DE STR MALDI-TOF instrument (Applied Biosystems) with a nitrogen laser in positive mode. The matrices used were sinapinic acid for protein samples and α-cyano-4-hydroxy-cinnamic acid (CHCA) for peptides. Matrices were prepared by mixing 15 mg of sinapinic acid or 10 mg of CHCA with 400 μL doubly distilled water, 100 μL of 3% TFA, and 500 μL of acetonitrile, followed by sonication for 3 min. Generally, 0.5 μL of protein or peptide samples were mixed with 0.5 μL of the appropriate matrix directly on the MALDI-TOF plate. The laser intensity was adjusted manually for each sample. Accurate mass spectra were recorded using a 12 T Apex-Qe FT-ICR mass spectrometer (Bruker Daltonics, Billerica, MA). Sample infusion was performed in positive-ion mode using a TriVersa NanoMate (Advion Biosciences, Ithica, NY) chip-based nanoelectrospray ionization (nanoESI) robot. The broad-band spectrum was acquired from 100 accumulations using a time domain data size of 512K words prior to Fourier transformation. The mass error between the most abundant isotope peak measured at 1693.09 *m*/*z* and the peak in the simulated pattern was 8 ppm. The mass of the cross-linked CFH∼7/tetrasaccharide conjugate was calculated as the individual masses of the free protein plus tetrasaccharide minus the one water molecule eliminated during cross-linking; all sulfates and the remaining carboxyl group in the GAG moiety were considered to be protonated.

Results

Titration of CFH∼7 with Fully Sulfated Heparin Tetrasaccharide Monitored by ^{1}H−^{15}N-HSQC. Combined chemical shift changes of backbone NH resonances at the end point of the CFH∼7 titration with tetrasaccharide are illustrated in Figure 1a. Residues with resonances most affected by binding are highlighted on the lowest-energy solution structure[33] of CFH∼7 in Figure 1b. Several of these are in close proximity to Y402, the residue whose variation is linked to AMD. CFH∼7 contains five lysines and four arginines that are also highlighted. Five of these basic residues are located toward the N-terminus, two occur within the middle of the module, and the two remaining are located close to the C-terminus. Only three (R404, K405, and K446) out of these nine residues had backbone NH ^{15}N and ^{1}H resonances significantly affected by the binding of the tetrasaccharide (Figure 1).

Dimerization of CFH∼7 Caused by Heparin Tetrasaccharide. As a consequence of the helical nature of heparin,[48−50] its negative charges are distributed on both faces of the helix and can be presented to proteins on either side. Indeed, a 1:2 GAG/protein complex has been observed for GAG fragments as short as tetrasaccharides (e.g., in the crystal structure of acidic fibroblast growth factor in complex with a fully sulfated heparin tetrasaccharide).[6] In solution, dimerization would be expected to slow down molecular tumbling and affect the ^{15}N NMR relaxation times. In the very fast monomer−dimer exchange approximation, no additional broadening of signals results from chemical exchange, thus the measured relaxation times should reflect the weighted average of the relaxation times of monomeric and dimeric species.[51] The majority of backbone NH signals of CFH∼7 exhibited marginal chemical shift changes

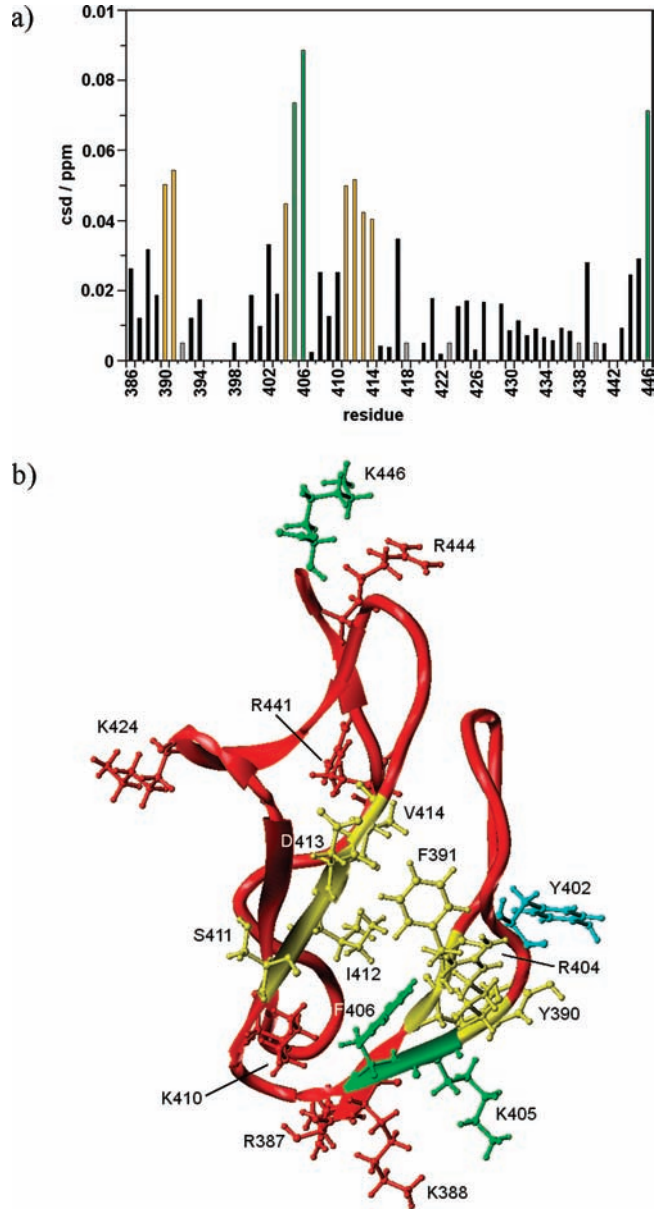

Figure 1. (a) Combined ^{1}H and ^{15}N chemical shift changes of CFH∼7 during ^{1}H−^{15}N-HSQC titrations (1:8 molar ratio of protein/carbohydrate) with fully sulfated heparin tetrasaccharide. Residues with chemical shift differences of 0.4−0.6 ppm or >0.6 ppm are highlighted in yellow or green, respectively. Nonobservable proline residues are shown in gray and given the arbitrary combined chemical shift difference of 0.005 ppm. (b) NMR structure of CFH∼7 (pdb entry 2JGX) showing in yellow or green residues highlighted in plot (a). AMD-associated residue 402 is shown in cyan. Side chains of the remaining basic residues are shown in red. The Figure was rendered using Sybyl (Tripos).

upon addition of tetrasaccharide, validating this approximation. The ^{15}N T_1 and T_2 relaxation times were measured[52] in a series of 1D experiments acquired at 800 MHz, and the rotational correlation time, τ_c, of CFH∼7 was determined using the R2R1 program (A. G. Palmer III, Columbia University). For free CFH∼7 and its complex with tetrasaccharide, these were measured to be 4.7 and 8.4 ns, respectively. Analogous data for the 402H isoform yielded τ_c values of 5.0 and 8.5 ns,

(48) Mulloy, B.; Forster, M. J. *Glycobiology* **2000**, *10*, 1147–1156.
(49) Zhang, Z.; Scott, A.; McCallum, J. X.; Nieto, L.; Corzana, F.; Jiménez-Barbero, J.; Chen, M.; Liu, J.; Linhardt, R. J. *J. Am. Chem. Soc.* **2008**, *130*, 12998–13007.
(50) Jin, L.; Hricovíni, M.; Deakin, J. A.; Lyon, M.; Uhrín, D. *Glycobiology* **2009**, *19*, 1185–1196.
(51) Roberts, G. C. K., Ed. *NMR of Macromolecules: A Practical Approach*; IRL Press at Oxford University Press: Oxford, U.K., 1993; p 164.
(52) Kay, L. E.; Nicholson, L. K.; Delagio, F.; Bax, A.; Torchia, D. *J. Magn. Reson.* **1992**, *97*, 359–375.

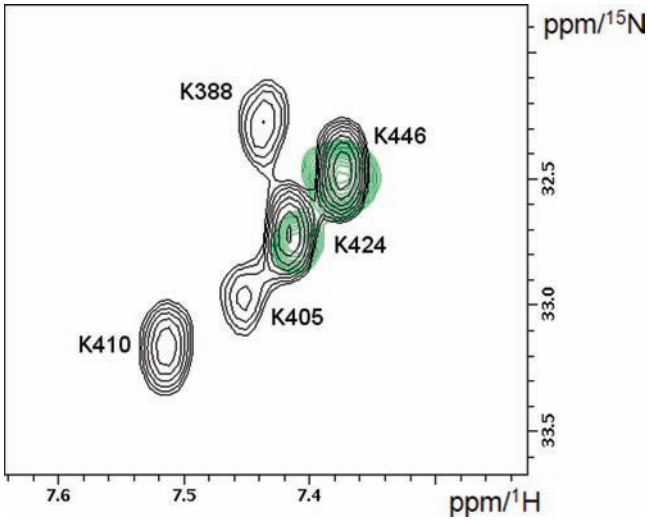

Figure 2. Superimposed $^1H-^{15}N$-HISQC spectra of the free (black) and cross-linked protein (green) at pH 3.0 and 283 K.

respectively. These data imply that binding to the heparin tetrasaccharide promotes the dimerization of both CFH∼7 variants.

Monitoring of Lysine and Arginine Side-Chain Resonances during Titrations. The lysine $N^{\zeta}H^{\zeta}{}_3{}^+$ signals are very rarely observed in standard $^1H-^{15}N$-HSQC spectra. This is because side-chain protons exchange rapidly with water under nearly physiological conditions and also N^{ζ} nuclei resonate approximately 90 ppm away from backbone nitrogen resonances and are inverted inefficiently by typical 80 μs ^{15}N pulses. Similarly, although to a lesser extent, $N^{\varepsilon}H^{\varepsilon}$ resonances of arginines are difficult to observe at neutral pH. It was demonstrated recently that refocusing of lysine $2H_3{}^+{}^{\zeta}{}_zN^{\zeta}{}_{x,y}$ coherences prior to the t_1 period allows the monitoring of $N^{\zeta}{}_{x,y}$ coherences in a HISQC experiment;[41] in-phase $N^{\zeta}{}_{x,y}$ coherences have longer relaxation times and are not quenched by exchange with water. Nevertheless, the HISQC experiment generally works well only if the exchange of H^{ζ} protons with water during the INEPT steps is slowed down by lowering the pH (2−4) and the temperature (5−15 °C). Under physiological conditions, $N^{\zeta}H^{\zeta}{}_3{}^+$ resonances were detected by the HISQC experiment only in the presence of stable salt bridges[53,54] or in protein complexes[41] where lysine side-chain NH atoms are protected from rapid exchange with water. In the case of CFH∼7, free or in complex with the tetrasaccharide, no lysine side-chain resonances were observed in the HISQC experiment under physiological conditions.

However, all five $N^{\zeta}H^{\zeta}{}_3{}^+$ cross-peaks appeared in the HISQC spectrum of free CFH∼7 (Figure 2) when the temperature was lowered to 283 K and the pH was adjusted to 3.0. A $^1H-^{15}N$-HSQC spectrum collected under these conditions confirmed that the protein was folded (data not shown). The $N^{\zeta}H^{\zeta}{}_3{}^+$ resonances were subsequently assigned through a comparison of the lysine side-chain carbon frequencies in 3D (H)CCENH$_3$[41] and (H)C(CO)NH-TOCSY[43] spectra (Figure 1S). Despite the fact that these spectra were acquired at different pH values, the match between individual CH chemical shifts was good, which is consistent with the remarkable stability of CCP modules.[55]

Unfortunately, the addition of tetrasaccharide to ^{15}N-labeled CFH∼7 at pH 3.0 and 283 K caused it to precipitate. We therefore decided to follow the complex formation at pH 7.4 and 298 K via the resonances of nonexchangeable lysine H^{ε}, C^{ε} (or N^{ζ}) side-chain atoms using a $^{15}N-^{13}C$-labeled sample. This was accomplished using the 3D H_2CN experiment[44] that uses the nonexchangeable H^{ε} protons for excitation and detection and indirectly monitors N^{ζ} and C^{ε} chemical shifts. Sufficient resolution was achieved by recording the $H^{\varepsilon}N^{\zeta}$ or $H^{\varepsilon}C^{\varepsilon}$ 2D planes rather than acquiring full 3D spectra. H_2CN spectra of the complex were assigned by recording the $H^{\varepsilon}N^{\zeta}$ plane of the H_2CN experiments on a free protein sample and comparing the ^{15}N chemical shifts with those obtained from the HISQC experiments. Both H_2CN planes were acquired during the course of a titration of CFH∼7 with tetrasaccharide. The $H^{\varepsilon}C^{\varepsilon}$ plane showed a better resolution of lysine resonances than did the $H^{\varepsilon}N^{\zeta}$ plane. Only two lysine residues (K405 and K388) exhibited significant chemical shift changes after the addition of tetrasaccharide (Figure 3a).

The same experiment also monitors the movement of arginine H^{δ}, C^{δ} (or N^{ε}) side-chain resonances, which appear as folded peaks when a small spectral width centered at 33 ppm is used in the indirectly detected ^{15}N dimension. The chemical shift perturbations of arginine $N^{\varepsilon}H^{\varepsilon}$ resonances were smaller than those of $H^{\varepsilon}N^{\zeta}$ of lysines, which can be explained by the fact that it is the quanidino group of arginines that is involved in the electrostatic interaction and not N^{ε}.[56] For arginine residues, the $H^{\delta}N^{\varepsilon}$ plane (Figure 3b) showed better resolution than did the $H^{\delta}C^{\delta}$ plane. Of the four arginine residues, only R404 has nonequivalent CH_2 protons. This residue exhibited the largest cross-peak movement during the titration. The second largest changes were observed for the $H^{\delta}N^{\varepsilon}$ resonances of R444, and the remaining two signals, belonging to R387 and R441, moved only very little.

Zero-Length Cross-Linking of Protein−GAG Complexes. Heparin tetrasaccharide was cross-linked to CFH∼7 as described in the Experimental Section. The products were separated by cation-exchange chromatography at pH 6.0 (Figure 4), and fractions were analyzed by positive-mode MALDI-TOF MS. Unlike the free protein that binds and is eluted with 0.3 M NaCl (7320.5 Da peak in Figure 4), the cross-linked CFH∼7/heparin tetrasaccharide conjugate, being more anionic, did not bind and was recovered in the flow-through. It yielded the strongest peak at 8378.4 Da with an M_r corresponding to CFH∼7 cross-linked to a single tetrasaccharide that has lost one sulfate group. A mass difference of 80 Da (equivalent to the mass of SO_3) between additional peaks indicated the further loss of sulfate groups during MS analysis. Minor compounds eluting at salt concentrations <0.3 M correspond to modifications of the free protein due to the remaining cross-linking reagent after the separation of the activated GAG. The peak with MW > 15 kDa is likely a product of protein−protein cross-linking.

Characterization of the Cross-Linked Conjugate by NMR and MS. A $^1H-^{15}N$-HSQC spectrum of the cross-linked CFH∼7-tetrasaccharide conjugate, recorded at 298 K and pH 6.0 (Figure 2S), exhibited an almost complete loss of signals from the N-terminal portion, as shown on the protein structure

(53) Tomlinson, J. H.; Ullah, S.; Hansen, P. E.; Williamson, M. P. *J. Am. Chem. Soc.* **2009**, *131*, 4674–4684.
(54) Poon, D. K.; Schubert, M.; Au, J.; Okon, M.; Withers, S. G.; McIntosh, L. P. *J. Am. Chem. Soc.* **2006**, *128*, 15388–15389.
(55) Kask, L.; Villoutreix, B. O.; Steen, M.; Ramesh, B.; Dahlbäck, B.; Blom, A. M. *Science* **2004**, *13*, 1356–1364.
(56) Fromm, J. R.; Hileman, R. E.; Caldwell, E. E. O.; Weiler, J. M.; Linhardt, R. J. *Arch. Biochem. Biophys.* **1995**, *323*, 279–287.

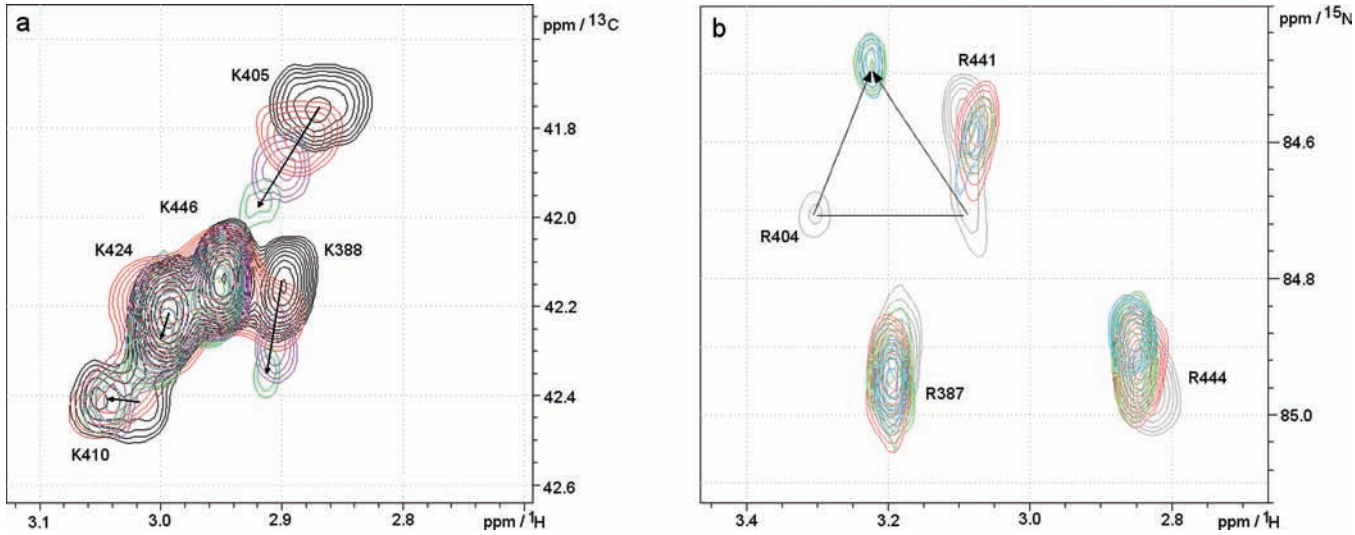

Figure 3. Lysine or arginine side-chain resonances monitored using the H_2CN experiment during the titration of CFH∼7 with heparin tetrasaccharide at pH 7.4 and 298 K. (a) $H^{\epsilon}C^{\epsilon}$ plane showing the lysine signals with protein/ligand ratios of 1:0 (black), 1:0.5 (red), 1:1 (purple), and 1:2 (green). (b) $H^{\delta}N^{\epsilon}$ plane showing the arginine signals with protein/ligand ratios of 1:0 (gray), 1:0.5 (red), 1:1 (green), and 1:2 (blue).

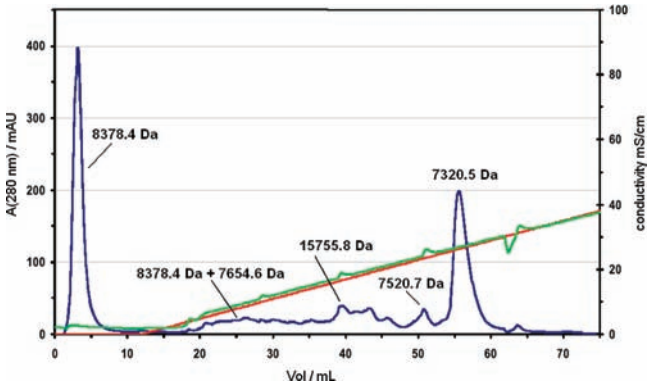

Figure 4. Cation-exchange chromatography at pH 6.0 of the reaction mixture after cross-linking CFH∼7 to fully sulphated heparin tetrasaccharide. Molecular masses of selected peaks were determined by MALDI-TOF MS.

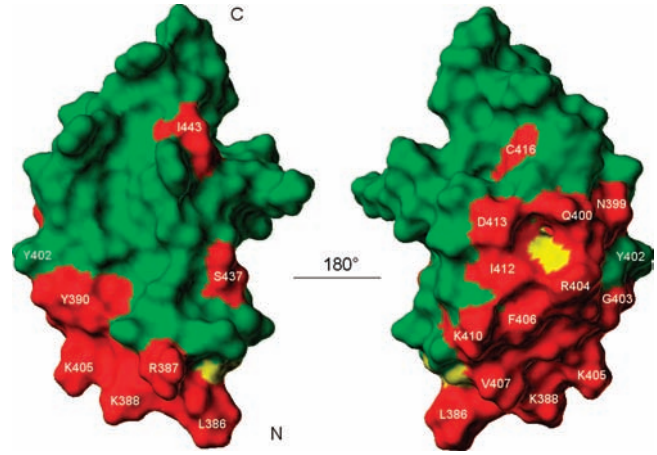

Figure 5. NMR structure of CFH∼7 (pdb entry 2JGX) showing residues whose NH backbone (red) or side-chain (yellow) resonances are missing in the $^1H-^{15}N$-HSQC spectrum of the cross-linked sample. The orientation of the molecule on the right is identical to that in Figure 1b. The Figure was rendered using Sybyl.

in Figure 5. Some of the remaining cross-peaks had distorted line shapes, but others were as sharp as those seen in the spectrum of the free protein. None of the three N-terminal lysine residues showed cross-peaks in the HISQC spectrum of the conjugate (Figure 2), but the K424 and K446 $N^{\zeta}H^{\zeta}{}_3{}^+$ cross-peaks were clearly visible and experienced almost no changes in chemical shifts or line widths.

Accurate FT-ICR-MS measurements confirmed that cross-linking produced a covalent 1:1 conjugate of tetrasaccharide and CFH∼7 with an M_r of 8460.5 Da. (Figure 6). ECD and in-source fragmentation resulted in progressive sulfate loss but not in significant protein fragmentation, confirming the stability of the cross-linked conjugate and the lability of NS/OS bonds. The high stability of the conjugate in MS-MS experiments is likely caused by the low largest-obtainable charge state (+5) and is a result of the presence of seven negative charges on the tetrasaccharide. Peptide analysis after trypsin digestion or chemical cleavage was therefore employed to investigate the site of the cross-linking.

Trypsin Digestion and Chemical Cleavage of the Cross-Linked Species. Because high concentrations (0.1 M) of DTT alone did not reduce the two disulfide bonds within CFH∼7, the complex was denatured by combined treatment with 8 M urea and 0.25 M DTT prior to alkylation with iodoacetamide. Successful reduction and alkylation was confirmed by MALDI-TOF MS. Protein fragments from the subsequent trypsin digestion, with MWs of 1470.6, 1879.7 and 2129.8 Da (Figure 3S), were identified as peptides S_{411}IDVACHPGYALPK$_{424}$, A_{425}QTTVTCMENGW-SPTPR$_{441}$, and K_{388}CYFPYLENGYNQNYGR$_{404}$ (theoretical masses of 1470.7, 1879.0, and 2129.3 Da, respectively). These fragments included lysine residues K388 and K424, indicating that these had not been modified by cross-linking. Additionally, the generation of the first of these peptides ($S_{411}-K_{424}$) suggests that K410 is also unmodified, because this residue is still recognized, and cleaved by trypsin.

Chemical fragmentation using TFA and microwave radiation[47] undertaken as a complementary approach yielded fragments that differed from those obtained using trypsin. The chemical cleavage effectively "sequenced" the C-terminus of the protein (Figure 4S) and established that K446 is also unmodified. In summary, the MS techniques directly showed that residues K388, K424, and K446 are not modified by cross-linking and implied that K410 also remains unmodified. Thus,

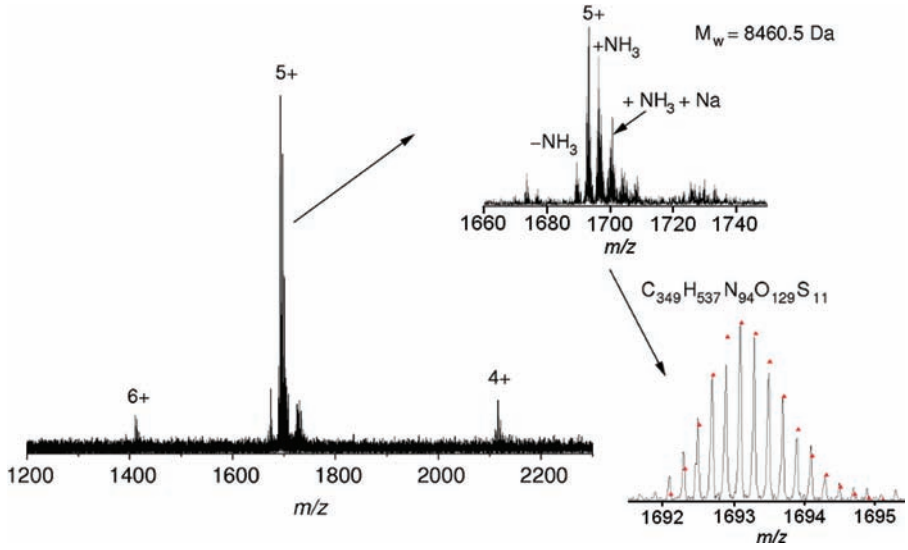

Figure 6. FTICR-MS spectrum of CFH∼7 cross-linked to fully sulfated heparin tetrasaccharide. A simulation of the isotope pattern for a charge state of +5 (red triangles) corresponds well to the measured main peak (black).

according to these experiments, K405 is the point of attachment of tetrasaccharide to CFH∼7 within the conjugate.

Discussion

Previous studies based on standard $^{1}H-^{15}N$-HSQC spectra identified two GAG-binding sites in CFH∼7 located near the C- and N-termini.[33,34] These sites may now be analyzed separately in light of the experimental results presented above. Four basic residues could potentially contribute to the binding at the C-terminus: K424, R441, R444, and K446. Of these, only R444 showed a significant movement of side-chain resonances in the titration experiments monitored by H_2CN spectra (Figure 3b). At the same time, backbone NH resonances of R444 remained relatively unperturbed. Inverse observations were made for K446, where backbone NH resonances were perturbed significantly upon titration but the side-chain resonances did not move at all (Figure 3a). The HISQC spectrum of the cross-linked species showed $N^{\zeta}H^{\zeta}_{3}{}^{+}$ cross-peaks of K424 and K446 that were also unchanged compared to the free protein. These observations were supported by MS analysis of the conjugate that identified peptide fragments containing unmodified lysines at these positions. We therefore infer that the side chain of R444 is the main contributor to charge−charge interactions at the C-terminal binding site whereas the K446 backbone amide forms a hydrogen bond to the tetrasaccharide. Involvement of the R444 side chain in the binding is in agreement with this side chain coordinating an SOS molecule in the crystal structure of the CFH∼6−8H−SOS complex.[34] Overall, the C-terminal binding site is weaker than the N-terminal one. This suggestion is supported by the limited movement of backbone and side-chain resonances and also by the lack of cross-linking of tetrasaccharide to this region of the protein.

Among the five basic residues of the N-terminal binding site of CFH∼7 (R387, K388, R404, K405, and K410), the H_2CN experiment identified side-chain resonances of K388, R404, and K405 as experiencing the largest chemical shift changes during titration with tetrasaccharide. Of these, K388 did not show a perturbation of the backbone NH cross-peaks whereas the other two residues did. The $^{1}H-^{15}N$-HSQC and HISQC spectra of the cross-linked conjugate lacked cross-peaks from residues in the N-terminal portion of the protein, which could be explained by an intermediate-timescale conformational exchange induced by the attachment of the tetrasaccharide (Figures 2 and 2S). MS analysis of the trypsin digest of the conjugate established that K388 and K410 were not modified, leaving only one lysine residue, K405, available for tetrasaccharide attachment. Combined MS and NMR data therefore allow us to locate the site of tetrasaccharide cross-linking to the side chain of K405.

Overall, we conclude that the side chains of K405, R404, and K388 provide most of the charge−charge interactions of the N-terminal HS/heparin binding site of CFH∼7. This is in agreement with mutagenesis studies that showed that mutations K405A and R404A significantly reduced heparin binding to CFH∼6−8.[57] The K388A mutation caused a smaller decrease in heparin affinity,[57] but in the context of a R387A/K388A double mutation,[58] the effects were substantial. A comparison of our solution data with the X-ray structure of the CFH∼6−8(H402)−SOS complex[34] is not straightforward for several reasons. The two studies use different proteins (triple- vs single-module and H402 vs the Y402 variant) and different ligands (SOS vs fully sulfated heparin tetrasaccharide). In the crystal structure of the CFH∼6−8 (H402)−SOS complex several CFH∼6−8 molecules contribute to the binding of each SOS molecule in an overall stoichiometry of 1:1. It seems possible that the observed arrangement in the protein crystal, prepared by cocrystallization, reflects the tendency of CFH∼6−8 to oligomerize in solution in the presence of a highly sulfated GAG mimic. This hypothesis is supported by our ^{15}N relaxation measurements that found increased self-association of both CFH∼7 variants in the presence of heparin tetrasaccharide. The X-ray structure shows hydrogen bonds between the sulfate and backbone NH of F391 in the immediate vicinity of Y402. This is consistent with the movement of NH backbone resonances Y390 and F391 observed in our titrations of CFH∼7 with the tetrasaccharide (Figure 1a).

Our data position the tetrasaccharide near the three basic residues K405, R404, and K388 and thus provide strong experimental evidence for its binding in close proximity to

(57) Clark, S. J.; Higman, V. A.; Mulloy, B.; Perkins, S. J.; Lea, S. M.; Sim, R. B.; Day, A. J. *J. Biol. Chem.* **2006**, *281*, 24713–24720.
(58) Giannakis, E.; Jokiranta, T. S.; Male, D. A.; Ranganathan, S.; Ormsby, R. J.; Fischetti, V. A.; Mold, C.; Gordon, D. L. *Eur. J. Immunol.* **2003**, *33*, 962–969.

Y402. This is in agreement with previous docking studies of a highly sulfated heparin pentasaccharide.[57] It was suggested previously that the mode of binding of SOS in the CFH∼6−8 (H402)−SOS complex[34] is incompatible with the position of the Y402 side chain found in the solution structure of CFH∼7 (Y402).[33] It is therefore likely that different sulfated molecules interact differently with the N-terminal binding site of CFH∼7. Differences were also observed in binding to Y402 and H402 of heparin species with various levels and patterns of sulfation.[57] More atomic -resolution data will be needed to explain these observations. Given the difficulties in crystallizing factor H modules in the presence of GAGs, NMR will play an important role in these investigations, which will benefit from the methodology outlined in this work.

Summarizing our findings from the methodological point of view, we have shown that the H_2CN experiment,[34] although requiring a double-labeled sample, is a very useful tool for monitoring lysine and arginine side-chain resonances of protein−GAG complexes under physiological conditions. The usefulness of the HISQC experiment is limited by the fact that it requires nonphysiological conditions. It can, however, provided useful information about covalently linked protein−GAG glycoconjugates.

Peptide analysis after trypsin digestion and chemical cleavage was employed to locate the cross-linking site. Four lysine residues out of five were shown, unambiguously, to be unmodified within a conjugate consisting of a tetrasaccharide moiety chemically cross-linked to a lysine side chain. It must therefore be the case that K405 is the site at which the tetrasaccharide is attached. No peptide containing the K405−tetrasaccharide conjugate could be detected by MALDI-TOF, presumably because of the large overall negative charge predicted for such a species. If the identification of a GAG−peptide construct were needed, then negative-ion ES-MS spectrometry would be an option.[21] Another potential hurdle to the positive identification of the conjugated proteolytic fragment, however, is that covalently attached oligosaccharides might compromise access by trypsin or Lys-C not just to the cleavage site directly following the conjugated lysine residue but also to nearby cleavage sites. This is likely to be a particular problem with GAG-binding proteins because they often contain clusters of lysine and arginine residues.

In a related zero-length cross-linking approach reported previously,[38] a GAG-binding protein was cross-linked to heparin immobilized on beads. The glycoconjugate was then subjected to proteolytic digestion on the beads, with subsequent identification of the cross-linked peptides by N-terminal sequencing, which gives a "gap" at the position of the cross-linked amino acid residue. This solid-phase assay requires immobilized GAGs, and only inhomogeneous heparin preparations are presently commercially available in this form. The authors of this approach also observed some cross-linking to arginines. This was not the case in our study because all arginine residues were recognized by trypsin and fragments containing unmodified arginines were also present in the chemically cleaved material. Our approach, being solution-based, can be equally applied to protein cross-linking to any type, size, or specific sequence of GAG oligosaccharides. Furthermore, whereas N-terminal protein sequencing is becoming increasingly less available, cross-linking in solution is more amenable to MS techniques, the application of which is rapidly evolving for GAGs.[59−61]

Conclusions

We have pointed out the shortcomings of the exclusive use of $^1H-^{15}N$-HSQC spectra for chemical shift mapping of GAG-binding sites on proteins. We found that the use of the HISQC experiment for monitoring chemical shift perturbations of side-chain amine groups is, in the case of a weak complex, limited to low pH and low temperature, although it is potentially useful for the analysis of cross-linked species. We demonstrated that the H_2CN experiment provides a more useful route for the characterization of the contributions of individual lysine and arginine side chains to ligand binding under physiological conditions. Furthermore, we showed that chemical cross-linking, as analyzed by proteolytic or chemical fragmentation and MS, provides a valuable complement to the NMR-based studies. By combining NMR and MS data, we inferred that two GAG-binding sites exist in CFH∼7 (Y402) in solution, with the R444 side chain and the K446 backbone amide being the dominant contributors to charge−charge interactions in the C-terminal binding site whereas the side chains of R404, K405, and K388 are most important for the N-terminal binding site that lies in the immediate vicinity of residue 402, which is implicated in AMD. The methods proposed here, using noncovalent complexes as well as a cross-linked protein−GAG conjugate, have the potential to aid structural investigations in the growing field of protein−GAG interactions.

Acknowledgment. This work was supported by the Wellcome Trust (078780/Z/05/Z to D.U.) and a CRUK Programme grant (M.L. and J.A.D.). We thank Stefan K. Weidt for acquiring the FT-ICR spectra.

Supporting Information Available: Details concerning the assignment of the resonances of lysine side chains, $^1H-^{15}N$ HSQC spectrum of the cross-linked CFH∼7, and MALDI-TOF spectra of peptides generated by trypsin digestion and microwave-assisted TFA-cleavage of the cross-linked complex. This material is available free of charge via the Internet at http://pubs.acs.org.

JA1000517

(59) Saad, O. M.; Leary, J. A. *Anal. Chem.* **2003**, *75*, 2985–2995.
(60) Saad, O. M.; Leary, J. A. *Anal. Chem.* **2003**, *75*, 5902–5911.
(61) Tissot, B.; Ceroni, A.; Powell, A. K.; Morris, H. R.; Yates, E. A.; Turnbull, J. E.; Gallagher, J. T.; Dell, A.; Haslam, S. M. *Anal. Chem.* **2008**, *80*, 9204–9212.